

Investigation on the Pyrolysis Kinetics and Mechanism of Date Stone Using Thermogravimetric Analysis

H. Hammani^{1,2}, W. Boumya¹, M. Achak³, O. Abdelaoui², M. El Achaby⁴, A. Barakat⁵, K. El harfi², M.A. El Mhammedi¹, A. Aboulkas^{2*}

¹Univ Hassan 1, Laboratoire de Chimie et Modélisation Mathématique, 25 000 Khouribga, Morocco.

²Laboratoire des procédés chimiques et matériaux appliqués (LPCMA), Faculté polydisciplinaire de Béni-Mellal, Université Sultan Moulay Slimane, BP 592, 23000 Béni Mellal, Morocco.

³Univ Chouaib Doukkali, Ecole Nationale des Sciences Appliquées, Laboratoire des Sciences de l'Ingénieur pour l'Energie, El Jadida, Morocco.

⁴Materials Science and Nanoengineering Department, Mohamed 6 Polytechnic University, Lot 660-Hay Moulay Rachid, 43150 Benguerir.

⁵IATE, CIRAD, Montpellier SupAgro, INRA, Université de Montpellier, 34060, Montpellier, France.

Abstract: The aim of this work was to investigate the physicochemical properties and thermal behavior of date stone in order to find an appropriate use of these materials for energy production. The physicochemical properties such as proximate analysis, ultimate analysis, heating values and FTIR spectroscopy of date stone were investigated. The pyrolytic characteristics and kinetics were investigated by thermogravimetric analysis. The experiments were performed in 105-900 °C temperature range under nitrogen atmosphere at heating rates of 5, 10, 20 and 50 °C/min. Pyrolysis characteristics were accomplished at four stages which can mainly be attributed to decomposition of extractives, decomposition of hemicellulose, decomposition of cellulose, and decomposition of lignin, respectively. Pyrolysis characteristics and the thermal decomposition rate were significantly affected by variation in the heating rate. However, the temperature peaks at maximum weight loss rate changed with increasing heating rate. The activation energy was obtained by model free methods proposed by Friedman (FR), Flynn-Wall-Ozawa (FWO) and Vyazovkin (VYA), and the kinetic mechanism was deduced by master plots method. The master plots method suggested that diffusion model was the most probable reaction mechanism to describe the pyrolysis of hemicellulose and the reaction model function was $g(x) = (1 - x) \ln(1 - x) + x$. The kinetic process for the decomposition process of cellulose can be described by reaction order model $g(x) = [(1 - x)^{-2} - 1]/2$. The results suggested that the experimental results and kinetic parameters provided useful information for the design of pyrolytic processing system using date stone as useful source of energy, chemicals and activated carbons.

Keywords: date stone; Pyrolysis; TGA-DTG; Kinetics; Master plots method.

1- Introduction

Due to the decrease in reservoir of fossil fuels and the increasing concerns on environmental protection, a great interest is focused on renewable energy sources. Among these sources, the biomass is widely regarded as a clean, sustainable, renewable and alternative energy source in the future. It is already the fourth largest energy source in the world, and it is widely dispersed. In this regard, biomass can be easily processed to produce chemicals and fuels since their reactivity and volatility are high [1]. In contrast to other renewable sources (e.g. solar, wind, hydro, geothermal) which can give heat and power, biomass offers a wide flexibility and can be converted into solid, liquid and gaseous fuel by applying suitable conversion technologies [2]. Thermochemical conversion technologies are advantageous over other conversion technologies in their ability to utilize almost all types of biomass and recovery of both energy and the chemical value of the feedstock.

Agricultural residues are a biomass which can be a sustainable energy source if its economic, environmental and social effects are properly managed. It may be a promising solution which does not interfere with the production of food and contribute to cover energy needs [3-5].

Annually in Morocco, a large amount of agricultural residues such as date stone is generated during process of date palm fruit. It is interesting to refer that date stone represents about one third of the date weight. These wastes are not utilized and can be utilized as an attractive energy source, preparing activated carbons or it can be converted into value-added chemical products [6,7]. However, the reuse of date stone helps to achieve the objectives of waste management and energy and chemicals recovery using thermochemical conversion processes. Among these, pyrolysis is at spotlight since it enables to produce energy fuels and chemicals recovery [8-11]. The biomass pyrolysis process can simply

be described as the thermal decomposition of biomass at moderate temperatures (400-600 °C) in the absence of oxygen to obtain preferably products (bio-oil, biochar or biogas). In order to use date stone for these applications, it is very important to investigate their thermal characteristic and kinetics.

Thermogravimetric analysis (TG) is the most common method used for kinetic analysis of pyrolysis process, and it provides a measurement of the mass loss of the sample with temperature and time. The kinetic data from TG are not only very useful for understanding the thermal degradation processes and mechanisms, but also can be used as input parameters for a thermal degradation reaction system. Extensive literature has been published on the experiments and mechanism aspects of a great range of biomass, such as olive residue, bagasse and date palm wastes [3,12–16]. H. Ceylan [12] studied the kinetics of the pyrolysis of plum stone using thermogravimetric analysis. Activation energy was determined using Friedman and Kissinger-Akahira-Sunose methods. They found a mean activation energy of 150 kJ/mol. Results of the Master-Plots method indicated that the most probable reaction model function was the *n*th order reaction model. Hani H. Sait et al. [3] investigated the kinetics of the pyrolysis and combustion of date palm biomass under non-isothermal conditions using thermogravimetric analysis. The highest degree of reaction and conversion was found within the temperature range of 200–450 °C. The activation energy was determined using Coats-Redfern method. The activation energies under inert and oxidative atmospheres were observed as 9.7–43.6 kJ mol⁻¹ and 9.04–30.95 kJ mol⁻¹. Y. El may et al. [14] determined activation energy for the thermal degradation of different date palm residues under inert and oxidative atmospheres using Coats-Redfern approach. The activation energy of date stone was observed to be 50.9 kJ mol⁻¹ and 57.7 kJ mol⁻¹ under inert and oxidative atmospheres, respectively.

From the literature review, we found out that there is no study on the description of the mechanism which controls the thermal decomposition of date stone. This fact motivated us to investigate the kinetics and mechanism of the pyrolysis of this waste. The aim of present study is to determine the physicochemical characterization of date stone such as proximate analysis, ultimate analysis, heating values and FTIR spectroscopy and to investigate the decomposition kinetics of date stone using the thermogravimetric analysis (TGA). In this sense, kinetic analysis was carried out by the application of the Friedman, Ozawa-Flynn-Wall and the Vyazovkin methods, which allow the calculation of the activation energy and masterplot method is employed in order to deduce the kinetic mechanism of the pyrolysis process.

2- Materials and Methods

2-1- Materials

The date stone, used in this study were collected from the factory in the region of Errachidia in Morocco. The date stone were washed with distilled water and dried at room condition. After drying, the stone were crushed and grinded into powdered form. The proximate and ultimate analysis of the date palm biomass has been presented in the Section 4.1.

2-2 Methods

Pyrolysis experiments were performed using thermogravimetric analyzer METTLER TOLEDO. To maintain pyrolysis conditions, high purity nitrogen was used as the carrier gas. In each test about 20 mg of sample was used. Each sample was heated to 105 °C and maintained at this temperature during 60 min to obtain the weight loss percentage associated with moisture. After the drying process, the sample was heated to 900 °C at heating rates of 5, 10, 20 and 50 °C/min under a nitrogen flow of 60 ml/min. The reproducibility of the experiments is acceptable and the experimental data presented in this paper corresponding to the different operating conditions are the mean values of runs carried out two or three times.

The possible chemical functional groups present in the date stone were investigated with the help of FT-IR technique (model bruker tensor 27) in the range of 400–4000 cm⁻¹ wavelength.

3- Kinetic modeling

The original mass loss versus temperature (TG) curves obtained at constant heating rate was transformed into the degree of conversion (*x*) versus temperature curves by means of the following equation:

$$x = \frac{w_0 - w}{w_0 - w_f} \quad (1)$$

where *w* is the weight of the sample at a given time *t*, *w*₀ and *w*_{*f*}, refer to values at the beginning and the end of the weight loss event of interest.

In kinetic analysis, it is generally assumed that the rate of heterogeneous solid-state reaction can be described by two separate functions *k*(*T*) and *f*(*x*) such that:

$$\frac{dx}{dt} = k(T) f(x) = A \exp\left(-\frac{E}{RT}\right) f(x)$$

k(*T*) is a temperature-dependent constant and *f*(*x*) is the reaction model, which describes the dependence of the reaction rate on the extent of reaction.

3.1 Isoconversional methods

3.1.1 Differential isoconversional method: Friedman method (FR) [17]

This method is a differential isoconversional method, and it directly based on Eq. (2) whose logarithm is

$$\ln\left(\frac{dx}{dt}\right) = \ln[Af(x)] - \frac{E}{RT} \quad (3)$$

From this equation, it is easy to obtain values for E over a wide range of conversions by plotting $\ln\left(\beta \frac{dx}{dT}\right)$ against

$$\frac{1}{T} \text{ for a constant } x \text{ value.}$$

3.1.2 Integral isoconversional method: Flynn-Wall-Ozawa method (FWO)[18–20]

The above rate expression can be transformed into non-isothermal rate expressions describing reaction rates as a function of temperature at a constant β ($\beta = dT/dt$):

$$\frac{dx}{dT} = \frac{1}{\beta} A \exp\left(-\frac{E}{RT}\right) f(x) \tag{4}$$

Integrating up to the conversion, x , Eq. (5) gives

$$g(x) = \int_0^x \frac{dx}{f(x)} = \frac{A}{\beta} \int_{T_0}^T \exp\left(-\frac{E}{RT}\right) dT \tag{5}$$

where $g(x)$ is the integral kinetic function or integral reaction model when its form is mathematically defined in Table 1.

One of the methods to obtain the E from dynamic data may be the one used by Flynn, Wall and Ozawa[18–21] using the Doyle’s approximation of $p(x)$ [22], which involves measuring the temperatures corresponding to fixed values of x from experiments at different heating rates. This is one of the integral methods that can determine the E which does not require the knowledge of reaction order.

$$\ln(\beta) = \ln\left[\frac{AE}{Rg(x)}\right] - 5.331 - 1.052 \frac{E}{RT} \tag{6}$$

Thus, for $x = const.$, the plot $\ln \beta$ vs. $\frac{1}{T}$, obtained from

thermograms recorded at several heating rates, should be a straight line whose slope can be used to evaluate the activation energy.

3.1.3 Integral isoconversional method: Vyazovkin (VYA)[23]

Another isoconversional method is the one developed by Vyazovkin and Lesnikovick[23] that allows both simple and complex reactions to be evaluated[24].

In Eq. (5), since $E/2RT \gg 1$, the temperature integral can be approximated by

$$\int_{T_0}^T \exp\left(-\frac{E}{RT}\right) dT \approx \frac{R}{E} T^2 \exp\left(-\frac{E}{RT}\right)$$

Substituting the temperature integral and taking the logarithm, we have that

$$\ln\left(\frac{\beta}{T^2}\right) = \ln\left[\frac{RA}{Eg(x)}\right] - \frac{E}{RT}$$

For each conversion value (x), $\ln(\beta/T^2)$ plotted versus $1/T$ gives a straight line with slope $-E/R$. Thus, E is obtained as a function of the conversion.

3.3. Masterplots method

It has been shown that universal master plots, valid for experimental data recorded under any heating profile, can be obtained by eq. (5):

$$g(x) = \frac{A}{\beta} \int_{T_0}^T \exp\left(-\frac{E}{RT}\right) dT = \frac{AE}{\beta R} P(u) \tag{9}$$

$P(u)$ is an exponential integral, $P(u) = \int_{\infty}^u -\left(\frac{e^{-u}}{u^2}\right) du$, where $u = E/RT$

Because $P(u)$ has no analytical solution, an approximation formula of high accuracy is used

(Doyle, 1962):

$$P(u) = 0.00484 \cdot \exp(-1.0516u) \tag{10}$$

Inserting $\alpha = 0.5$ into Eq. (9), one can get:

$$g(0.5) = \left(\frac{AE}{\beta R}\right) P(u_{0.5}) \tag{11}$$

Where $u_{0.5} = E/RT_{0.5}$, $T_{0.5}$ is the temperature when $x = 0.5$.

When Eq. (9) is divided by Eq. (11), the following equation is obtained:

$$\frac{g(x)}{g(0.5)} = \frac{P(u)}{P(u_{0.5})} \tag{12}$$

Eq. (12) shows that for a given x , the reduced-generalized reaction rate, $P(u)/P(u_{0.5})$, is equivalent to $g(x)/g(0.5)$ if

the proper $g(x)$ is considered (details can be found in [25,26]). The equation above implies that, for experimental data recorded under non-isothermal conditions, the knowledge of the activation energy is required to construct the experimental master plots. The suitable pyrolysis reaction mechanisms are obtained by comparing the experimental $(P(u)/P(u_{0.5}))$ and theoretical $(g(x)/g(0.5))$ curves.

Table 1: Set of reaction models applied to describe the reaction kinetics in heterogeneous solid state systems.

Model		Differential form $f(x) = \frac{1}{k} \frac{dx}{dt}$	Integral form $g(x)$
Nucleation models			
Power law	P2	$2x^{1/2}$	$x^{1/2}$
Power law	P3	$3x^{2/3}$	$x^{1/3}$
Power law	P4	$4x^{3/4}$	$x^{1/4}$

“Investigation on the Pyrolysis Kinetics and Mechanism of Date Stone Using Thermogravimetric Analysis”

Avarami-Erofeyev	A2	$2(1-x)[- \ln(1-x)]^{1/2}$	$[- \ln(1-x)]^{1/2}$
Avarami-Erofeyev	A3	$3(1-x)[- \ln(1-x)]^{2/3}$	$[- \ln(1-x)]^{1/3}$
Avarami-Erofeyev	A4	$4(1-x)[- \ln(1-x)]^{3/4}$	$[- \ln(1-x)]^{1/4}$
Geometrical contraction models			
Contracting area	R2	$2(1-x)^{1/2}$	$[1-(1-x)^{1/2}]$
Contracting volume	R3	$3(1-x)^{2/3}$	$[1-(1-x)^{1/3}]$
Diffusion models			
1-D diffusion	D1	$1/2x$	x^2
2-D diffusion	D2	$[- \ln(1-x)]^{-1}$	$[(1-x) \ln(1-x)] + x$
3-D diffusion, Jander	D3	$3(1-x)^{2/3} / [2(1-(1-x)^{1/3})]$	$[1-(1-x)^{1/3}]^2$
Ginstling-Brounshtein	D4	$3/[2((1-x)^{-1/3} - 1)]$	$1 - (2x/3) - (1-x)^{2/3}$
Reaction-order models			
First-order	F1	$(1-x)$	$- \ln(1-x)$
Second-order	F2	$(1-x)^2$	$(1-x)^{-1} - 1$
Third-order	F3	$(1-x)^3$	$[(1-x)^{-2} - 1]/2$

4- Results and discussion

4-1 Physico-chemical characteristics

The proximate and ultimate analysis of date stone is given in Table 2. It was observed that date stone are rich in carbon and oxygen contents (43.81-46.9%). The composition showed approximately 0.45 % of nitrogen and 0.19% of sulfur. Biomass with low nitrogen and sulfur contents are attractive to thermochemical conversion processes because high N and S contents will lead to more toxic NO_x and SO₂ emission [27].

As depicted in Table 2, date stone are in high volatile contents (73.46 %) that could be considered suitable for pyrolysis, gasification or combustion processes [3,28]. The ash contents are low, about 2.24 %. Comparison with

literature data for date stone shows that the investigated date stone have very low levels of ash [3,12]. Low ash content features suggest that they can be regarded as suitable feedstocks for pyrolysis process, since lower ash content of feedstock takes the advantages to lower fouling or aggregation on reactors.

The knowledge of the ratios of H/C and O/C is more important for thermochemical conversion processes. In most cases, biomasses are higher O/C and H/C ratios than the fossil fuels. The high values of the atomic H/C ratio (1.64) in date stone agree with the high volatile content found by proximate analysis (73.46 %). The values obtained for these parameters are relatively similar to those reported for date stone in the literature [3,12,14].

Table 2: Physico-chemical characteristics of date stone.

Proximate analyses (wt.%)				Ultimate analyses (wt.%)					HHV(kJ/kg)	H/C	O/C
Moisture	Volatile matter	Fixed carbon	Ash	C	H	O	N	S			
6.59	73.46	24.3	2.24	46.9	6.41	43.81	0.45	0.19	18.77	1.64	0.70

The infra-red analysis of spectroscopy was employed to identify the component of date stone. The FTIR spectrum obtained is given in Fig. 1. The spectra revealed intense peak at 3320 cm⁻¹ that represents the O-H absorption mainly indicating the presence of alcohols, phenols, carboxylic acids or water. The peaks between 3000 and 2800 cm⁻¹ correspond to C-H absorption due to CH₂ and CH₃ asymmetric and symmetric stretching vibrations. These vibrations are expected from hemicellulose, cellulose and

lignin [29]. The peak at 1740 cm⁻¹ is attributed to the stretching mode of C=O in hemicelluloses [30]. The peak at 1600 cm⁻¹ is assigned to the COO⁻ asymmetric stretching vibration in acidic groups of pectic polysaccharides and lignin [31,32].

The peak at 1515 cm⁻¹ was assigned to C=C phenolic stretch of guaiacyl ring of lignin [32]. The peaks at 1438 and 1372 cm⁻¹ were assigned to C-H bends from asymmetric and symmetric CH₃ of polysaccharides and cellulose. The peak

at 1236 cm^{-1} was assigned to a C-C plus C-O plus C=O stretch[32]. The very intense peak at 1035 cm^{-1} was assigned to a C-O-C asymmetric stretching vibration, and, along with peaks at 1147 and 1102 cm^{-1} , they are related to hemicellulose. It could be determined that date stone include oxygen groups, carbonyl groups, ethers, esters, alcohols, and phenol groups.

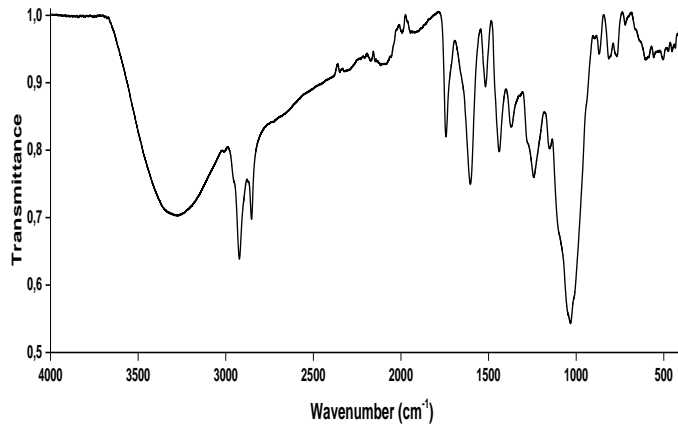


Figure 1: FTIR spectra of date stone

4-2 Thermal decomposition characteristic

The thermogravimetric (TG) and DTG curves of the date stone at heating rate of 5, 10, 20 and 50 °C/min were exhibited in Fig.2. The pyrolysis process can be divided into three stages since every single slope change on a TG curve indicates the beginning of a new stage: hemicellulose, cellulose and finally lignin or char. Typically, the thermal decomposition of biomass is given as: hemicellulose, cellulose and lignin[13,33]. Generally, the main thermal decomposition of lignocellulosic materials occurs over the temperature range of 200-400 °C[13,15,34]. By considering the TG curve obtained at 10 °C min⁻¹, it is apparent that date stone show a mass loss (4.68 %) which finishes at approximately 220 °C. This mass loss can be attributed to the extractives in date stone. Extractives are compounds with low molecular mass as compared to cellulose, and may promote ignitability of the biomass at lower temperatures as a result of their higher volatility and thus accelerate the degradation process[35,36].

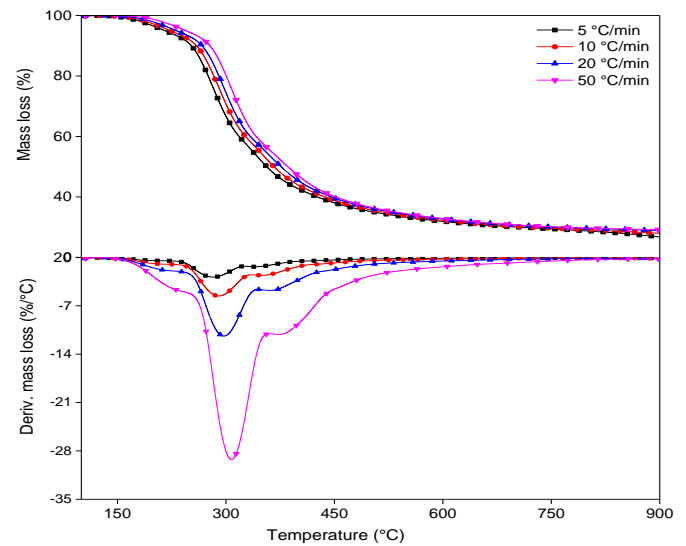


Figure 2: TG and DTG curves of date stone at different heating rates.

From this point on, three components of date stone, hemicelluloses, cellulose and lignin, started to decompose as the temperature increased. The main pyrolysis (where the main degradation occurred) starts at 220 °C and ends at approximately 400 °C. During this main degradation stage, the date stone had the highest weight loss, which was about 52 % of the total weight loss. This main devolatilization was attributed to a sharp drop in mass loss curve and formation of the main thermal degradation product, corresponding to the degradation of hemicellulose and cellulose[13,15,33,34]. The peak of cellulose decomposition is concealed by that of hemicellulose, while the temperature demarcation for cellulose decomposition is overlapped with that of hemicellulose which dominates the thermal decomposition of date stone. These peaks were identified at 291 °C and 352 °C for degradation of hemicellulose and cellulose respectively.

After the main devolatilization, there was a gradual drop in weight loss. This phenomenon could be explained by the decomposition process of remaining solid residues or char, which increased until 900 °C. This continuous slight devolatilization can be attributed to the slow degradation of lignin. The mass loss rate of this stage is much lower compared to those in the first and second stages. The mass loss occurred in this stage was 16.03% and the char at the end of the overall pyrolysis process was determined as 27.97 %. The decomposition of cellulose and hemicellulose cause the formation of organic volatiles, whereas devolatilization of lignin enhances the formation of char.

It is known that the hemicelluloses decompose before cellulose and lignin and[3,12,33]. Yang et al.[33] reported the temperature ranges for decomposition of hemicellulose, cellulose and lignin as, 220-315 °C, 315-400 °C and 160-900 °C, respectively. The results of this study were in agreement with reported temperature intervals. Hani H. Sait et al.[3] cited that the main devolatilization of date palm biomasses starts at 200 °C and can be completely at 400

°C, was attributed due to release of volatile matter. S. Ceylan[12] studied the non-isothermal degradation of plum stone waste by thermogravimetric analysis. They cited that the main degradation of plum stone takes place between 175-362°C. In this temperature range, most of the cellulose and hemicellulose in the sample were degraded and volatilized. Y. El may et al.[14] confirmed that the hemicelluloses degrade between 170 and 280°C, the cellulose degrades between 280 and 340 °C, and the degradation of lignin takes place between 340 and 500 °C. The stages of thermal behavior are associated with the components of date stone; which mainly consists of hemicellulose, cellulose and lignin as with all other lignocellulosic biomasses.

The heating rate played an important role in determining the characteristic temperatures of different stages and events as shown in Table 3. The DTG curves for the pyrolysis of date stone at different heating rates of 5, 10, 20 and 50 °C min⁻¹ are shown in Fig. 2. An increase of the heating rate tended to delay thermal degradation processes towards higher temperatures, most probably due to increased thermal lag as at a given temperature a higher heating rate implies that the material reaches that temperature in a shorter time [13,15,16]. On the other hand, the pyrolysis reactions can affect the heat transfer in particle. The release of volatiles leads to the formation of char which is in poor heat transfer performance and prevents the heat transfer into particle core to some extent. However, at high heating rates separate peaks do not arise because some of them are decomposed simultaneously, and several adjacent peaks are united to form overlapped broader and higher peaks. Furthermore, during the analysis, at low heating rate, a larger instantaneous thermal energy is provided to the system and a longer time may be required for the purge gas to reach equilibrium with the temperature of the furnace of the sample. While at the same time and in the same

temperature region a higher heating rate has a short reaction time and therefore the temperature needed for the sample to decompose is also higher. This causes the maximum rate curve to shift to the right [37].

Table 3: Different temperature values of the date stone.

Heating rate (°C min ⁻¹)	Hemicellulose (°C)	Cellulose (°C)
	T _I / T _{max} / T _F	T _I / T _{max} / T _F
5	224 / 223 / 326	326 / 340 / 400
10	232 / 291 / 334	334 / 352 / 414
20	239 / 298 / 343	343 / 362 / 426
50	253 / 308 / 356	356 / 380 / 440

4-3 Thermal degradation kinetics

The results of TG/DTG experimental data of date stone pyrolysis obtained in the temperature regions of 200-400°C were used for kinetic analysis. This Kinetic analysis results is limited to the stages of the pyrolysis of hemicellulose and cellulose. The isoconversional method adopted to analyze the pyrolysis could eliminate the influence of the mechanism function of uncertainty on activation energy. Friedman (FR), Flynn-Wall-Ozawa (FWO) and Vyazofkin (VYA) methods were used to determine the activation energies. Linear regression was used to obtain the values of activation energies in terms of $x = 0.2 - 0.8$ with an increment of 0.05 for each stage (hemicellulose and cellulose). The results on the activation energies for hemicellulose and cellulose degradation of date stone calculated from the slope of three isoconversional methods are reported in Table 4. In most cases, we observed excellent fitting goodness with R² values above 0.99. The dependence of apparent activation energy (E) on the degree of conversion (x) (E-x curve) for decomposition process of hemicellulose and cellulose obtained by isoconversional methods is presented in Figs. 3a and 3b, respectively.

Table 4: Activation energy (E) deduced from the FR, FWO and VYA isoconversional methods.

conversion x	Hemicellulose			cellulose		
	E _a (Kj/mol)			E _a (Kj/mol)		
	FR	OFW	VYA	FR	OFW	VYA
0,2	110,94	137,90	139,38	189,94	182,13	185,53
0,25	118,28	149,51	151,43	184,20	182,13	185,48
0,3	123,81	137,90	139,62	189,71	182,13	185,49
0,35	119,02	149,51	151,25	177,61	182,13	185,42
0,4	125,82	137,90	139,54	187,40	182,13	185,45
0,45	126,77	137,90	139,56	190,29	197,94	201,16
0,5	135,88	137,90	139,49	185,94	197,94	201,00
0,55	145,47	149,51	151,25	181,78	197,94	200,99
0,60	142,27	149,51	151,00	182,81	197,94	190,99

0,65	140,38	149,51	151,27	166,92	197,94	199,87
0,7	145,62	137,90	139,60	160,57	197,94	199,42
0,75	143,74	150,86	155,65	165,47	197,94	198,84
0,8	148,43	149,51	151,30	164,67	197,94	197,70
Mean	132,80±13	144,26±7	146,18±7	179,02±11	191,86±8	193,64±8

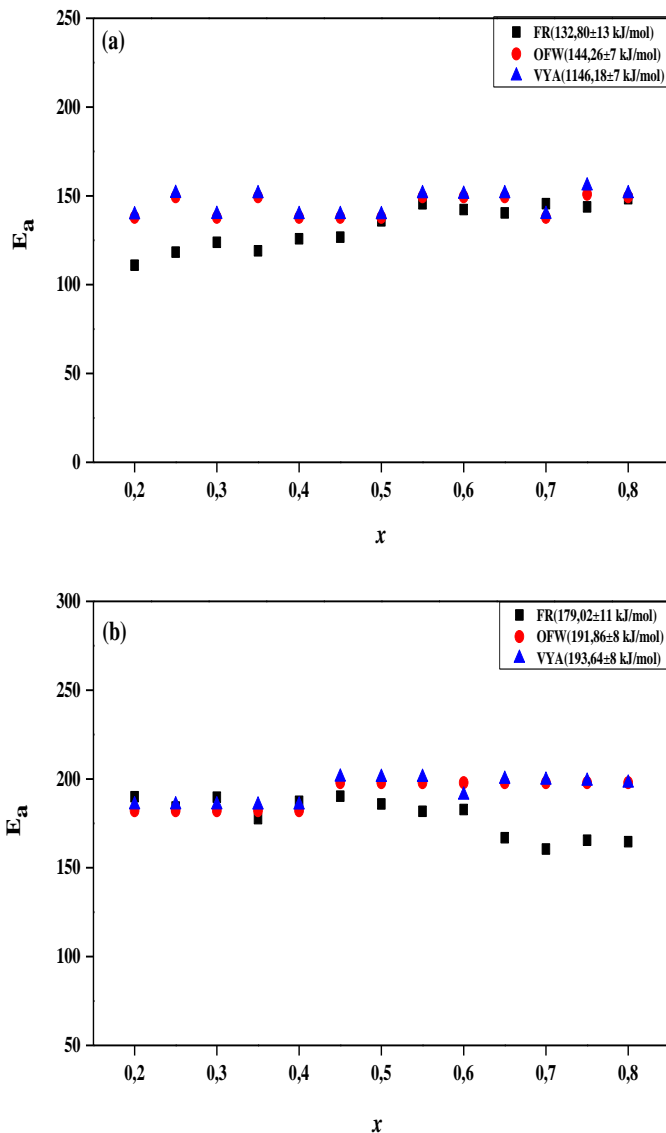


Figure 3: Activation energy distribution at different conversion rates (x) for degradation of hemicellulose (a) and cellulose (b) in date stone determinate during FR, FWO and VYA isoconversional methods

The mean activation energies calculated for hemicellulose by FR, FWO and VYA methods were 132.80 ± 13 , 144.26 ± 7 and 146.18 ± 7 kJ mol^{-1} , respectively. The value of activation energy is about 179.02 ± 11 , 191.86 ± 8 and 193.64 ± 8 kJ mol^{-1} for the cellulose degradation by FR, FWO and VYA methods, respectively. This result indicated that the activation energy of hemicellulose is lower than that of

cellulose. It is well-known that the hemicellulose is the least thermally stable of the biomass components, and therefore, its activation energy in an inert thermal decomposition process is lower than the cellulose one. The cellulose is very stable links, thus requiring more energy for the decomposition.

In comparison with the literature for different date palm biomasses, Ceylan[12] investigated pyrolysis kinetics of plum stone waste using model-free methods, and determined activation energy for stage $x = 0.1-0.65$ (hemicellulose) is $150.7 \text{ kJ mol}^{-1}$ and $193.22 \text{ kJ mol}^{-1}$ for stage $x = 0.7-0.8$ (cellulose). These results agree with our study. Y. El maya et al.[14] used TGA to investigate thermal behaviour of different date palm residues under inert and oxidative atmospheres, and reported activation energy of date stone pyrolysis as 50.9 kJ mol^{-1} and 57.7 kJ mol^{-1} (obtained by Coats-Redfern method) under inert and oxidative atmospheres, respectively. H.H. Sait et al.[3] studied the pyrolysis kinetics of date palm biomass using Coats-Redfern method. They reported activation energies under inert and oxidative atmospheres between $9.7-43.6 \text{ kJ mol}^{-1}$ and $9.04-30.95 \text{ kJ mol}^{-1}$ (obtained by Coats-Redfern method), respectively. The reported values using Coats-Redfern method were lower than the results of our study.

As it can be seen in Table 4 and Fig. 3 all three methods predict the same trend of dependence of the activation energy on the extent of degradation. As it was also noted the results from the two integral methods, i.e., FWO and VYA are almost identical, while those from the Friedman method are shifted to low values. It has been claimed that this steady difference can be explained by the different approximations used to calculate the temperature in these method. The differential method employs instantaneous rate values which are more likely to be sensitive to experimental noise. In addition, the integral methods assume a constant activation energy thus introducing a systematic error when E varies with x .

As said previously, the knowledge of x as a function of temperature and the value of the activation energy are essential in order to calculate the experimental masterplots against x from experimental data obtained under heating rate (Eq. (12)). Using the predetermined value of $E = 141.08 \text{ kJ mol}^{-1}$ (mean activation energy obtained the FWO, VYA and FR methods), along with the temperature measured as a function of a under various heating rates, the experimental

master plots for TGA data of date stone was constructed according to Eq. (12). Figs. 4 and 5 show the experimental masterplots against x constructed from experimental data under different heating rates. The theoretical masterplots corresponding to the $f(x)$ functions in Table 1 are also shown in Figs. 4 and 5. It is shown that the all experimental masterplots of decomposition process of hemicellulose at 5, 10, 20 and 50 °C min⁻¹ are consistent with theoretical masterplot for D₂ kinetic models. For degradation of cellulose, the comparison of the experimental masterplots with theoretical ones indicates that the kinetic process be most probably described by F₃ model.

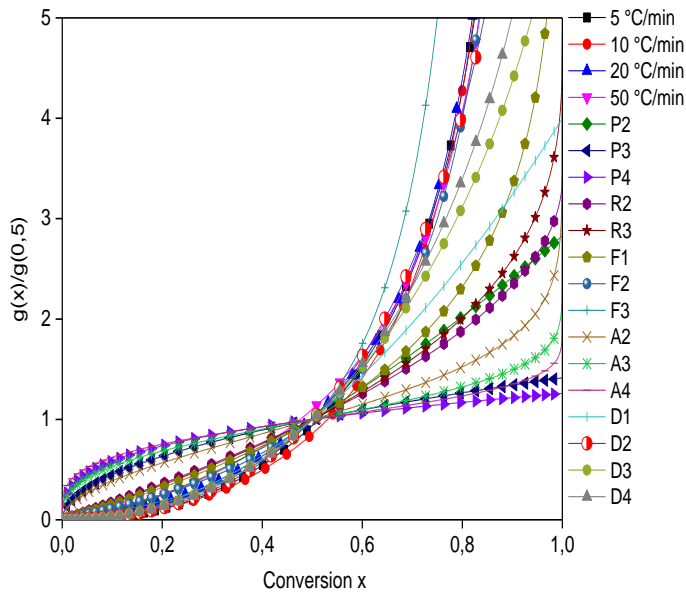


Figure 4: Theoretical masterplots of $g(x)/g(0.5)$ vs x and the experimental masterplot for degradation of hemicellulose.

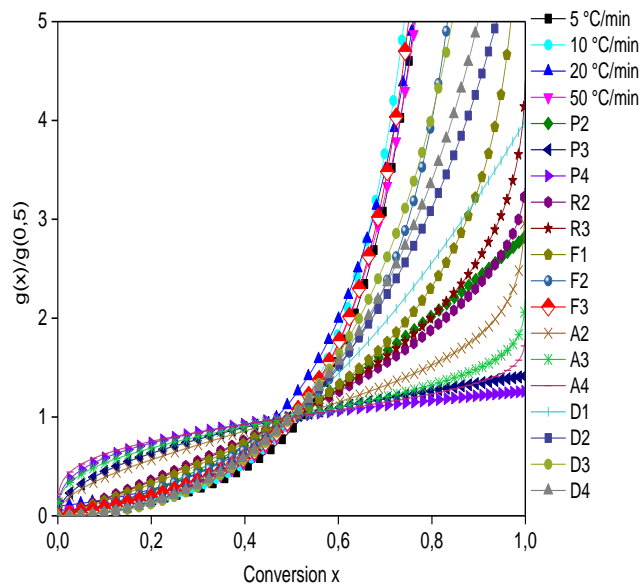


Figure 5: Theoretical masterplots of $g(x)/g(0.5)$ vs x and the experimental masterplot for degradation of cellulose.

5- Conclusion

In this work, date stone was pyrolyzed in a TG analyzer from 105 to 900 °C at different heating rates of 5, 10, 20 and 50 K/min. The results indicated that the pyrolysis process contains three stages, mainly corresponds to hemicelluloses, cellulose and lignin decomposition, respectively. It was found that TG and DTG curves tended to shift to a greater range of temperatures as the heating rates increased, causing the maximum curve rate to spread to the right. The activation energy of date stone was calculated using isoconversional methods such as Friedman (FR), Ozawa-Flynn-Wall (OFW) and Vyazofkin (VYA) methods. The mean activation energies for degradation of hemicellulose were 132.80±13, 144.26±7 and 146.18±7 kJ mol⁻¹, respectively. The mean value of activation energy is about 179.02±11, 191.86±8 and 193.64±8 kJ.mol⁻¹ for the cellulose degradation, respectively. The most probable reaction mechanisms were described by D₂ and F₂ kinetic models for degradation of hemicellulose and cellulose, respectively.

References

1. M. Esen, T. Yuksel, Experimental evaluation of using various renewable energy sources for heating a greenhouse, *Energy Build.* 65 (2013) 340–351. doi:10.1016/j.enbuild.2013.06.018.
2. Energy for the Future: Renewable Sources of Energy. White Paper for a Community Strategy and Action Plan. COM (97) 599 final, 26 November 1997 [follow-up to the Green Paper], (1997). <http://aei.pitt.edu/1130/> (accessed November 12, 2016).
3. H.H. Sait, A. Hussain, A.A. Salema, F.N. Ani, Pyrolysis and combustion kinetics of date palm biomass using thermogravimetric analysis, *Bioresour. Technol.* 118 (2012) 382–389. doi:10.1016/j.biortech.2012.04.081.
4. N. Grioui, K. Halouani, F.A. Agblevor, Bio-oil from pyrolysis of Tunisian almond shell: Comparative study and investigation of aging effect during long storage, *Energy Sustain. Dev.* 21 (2014) 100–112. doi:10.1016/j.esd.2014.05.006.
5. M. Jeguirim, J. Bikai, Y. Elmay, L. Limousy, E. Njeugna, Thermal characterization and pyrolysis kinetics of tropical biomass feedstocks for energy recovery, *Energy Sustain. Dev.* 23 (2014) 188–193. doi:10.1016/j.esd.2014.09.009.
6. M. Belhachemi, R.V.R.A. Rios, F. Addoun, J. Silvestre-Albero, A. Sepúlveda-Escribano, F. Rodríguez-Reinoso, Preparation of activated carbon from date pits: Effect of the activation agent and liquid phase oxidation, *J. Anal. Appl. Pyrolysis.* 86 (2009) 168–172. doi:10.1016/j.jaap.2009.05.004.
7. M.U.H. Joardder, M.S. Uddin, M.N. Islam, The Utilization of Waste Date Seed as Bio-Oil and

- Activated Carbon by Pyrolysis Process, *Adv. Mech. Eng.* 4 (2015) 316806–316806. doi:10.1155/2012/316806.
8. A. Aboulkas, T. Makayssi, L. Bilali, K. El harfi, M. Nadifiyine, M. Benchanaa, Co-pyrolysis of oil shale and plastics: Influence of pyrolysis parameters on the product yields, *Fuel Process. Technol.* 96 (2012) 209–213. doi:10.1016/j.fuproc.2011.12.001.
 9. A. Aboulkas, T. Makayssi, L. Bilali, K. El harfi, M. Nadifiyine, M. Benchanaa, Co-pyrolysis of oil shale and High density polyethylene: Structural characterization of the oil, *Fuel Process. Technol.* 96 (2012) 203–208. doi:10.1016/j.fuproc.2011.12.003.
 10. F. Mushtaq, T.A.T. Abdullah, R. Mat, F.N. Ani, Optimization and characterization of bio-oil produced by microwave assisted pyrolysis of oil palm shell waste biomass with microwave absorber, *Bioresour. Technol.* 190 (2015) 442–450. doi:10.1016/j.biortech.2015.02.055.
 11. J.E. Omoriyekomwan, A. Tahmasebi, J. Yu, Production of phenol-rich bio-oil during catalytic fixed-bed and microwave pyrolysis of palm kernel shell, *Bioresour. Technol.* 207 (2016) 188–196. doi:10.1016/j.biortech.2016.02.002.
 12. S. Ceylan, Kinetic analysis on the non-isothermal degradation of plum stone waste by thermogravimetric analysis and integral Master-Plots method, *Waste Manag. Res.* 33 (2015) 345–352. doi:10.1177/0734242X15574590.
 13. M.Y. Guida, H. Bouaik, A. Tabal, A. Hannioui, A. Solhy, A. Barakat, A. Aboulkas, K.E. Harfi, Thermochemical treatment of olive mill solid waste and olive mill wastewater, *J. Therm. Anal. Calorim.* 123 (2015) 1657–1666.
 14. M. Jeguirim, S. Dorge, G. Trouvé, R. Said, others, Study on the thermal behavior of different date palm residues: characterization and devolatilization kinetics under inert and oxidative atmospheres, *Energy.* 44 (2012) 702–709.
 15. A. Ounas, A. Aboulkas, K. El harfi, A. Bacaoui, A. Yaacoubi, Pyrolysis of olive residue and sugar cane bagasse: Non-isothermal thermogravimetric kinetic analysis, *Bioresour. Technol.* 102 (2011) 11234–11238.
 16. E. Ozgur, S.F. Miller, B.G. Miller, M.V. Kok, Thermal analysis of co-firing of oil shale and biomass fuels, *Oil Shale.* 29 (2012) 190–202.
 17. H.L. Friedman, Kinetics of thermal degradation of char-forming plastics from thermogravimetry. Application to a phenolic plastic, *J. Polym. Sci. Part C Polym. Symp.* 6 (1964) 183–195. doi:10.1002/polc.5070060121.
 18. J.H. Flynn, L.A. Wall, A quick, direct method for the determination of activation energy from thermogravimetric data, *J. Polym. Sci. [B].* 4 (1966) 323–328. doi:10.1002/pol.1966.110040504.
 19. J.H. Flynn, L.A. Wall, General treatment of the thermogravimetry of polymers, *J Res Nat Bur Stand.* 70 (1966) 487–523.
 20. T. Ozawa, A New Method of Analyzing Thermogravimetric Data, *Bull. Chem. Soc. Jpn.* 38 (1965) 1881–1886. doi:10.1246/bcsj.38.1881.
 21. T. Ozawa, Kinetic analysis of derivative curves in thermal analysis, *J. Therm. Anal. Calorim.* 2 (1970) 301–324. doi:10.1007/BF01911411.
 22. C.D. Doyle, Kinetic analysis of thermogravimetric data, *J. Appl. Polym. Sci.* 5 (1961) 285–292. doi:10.1002/app.1961.070051506.
 23. S. Vyazovkin, A.I. Lesnikovick, Transformation of “degree of conversion against temperature” into “degree of conversion against time” kinetic data, *Russ J Phys Chem.* 62 (1988) e7.
 24. S. Vyazovkin, N. Sbirrazzuoli, Confidence intervals for the activation energy estimated by few experiments, *Anal. Chim. Acta.* 355 (1997) 175–180.
 25. F.J. Gotor, J.M. Criado, J. Malek, N. Koga, Kinetic Analysis of Solid-State Reactions: The Universality of Master Plots for Analyzing Isothermal and Nonisothermal Experiments, *J. Phys. Chem. A.* 104 (2000) 10777–10782. doi:10.1021/jp0022205.
 26. J. Criado, L. Pérez-Maqueda, F. Gotor, J. Málek, N. Koga, A unified theory for the kinetic analysis of solid state reactions under any thermal pathway, *J. Therm. Anal. Calorim.* 72 (2003) 901–906. doi:10.1023/A:1025078501323.
 27. A.K. Varma, P. Mondal, Physicochemical characterization and kinetic study of pine needle for pyrolysis process, *J. Therm. Anal. Calorim.* 124 (2016) 487–497.
 28. A. Demirbas, Combustion characteristics of different biomass fuels, *Prog. Energy Combust. Sci.* 30 (2004) 219–230.
 29. S. Naik, V.V. Goud, P.K. Rout, K. Jacobson, A.K. Dalai, Characterization of Canadian biomass for alternative renewable biofuel, *Renew. Energy.* 35 (2010) 1624–1631.
 30. R. Briones, L. Serrano, R.B. Younes, I. Mondragon, J. Labidi, Polyol production by chemical modification of date seeds, *Ind. Crops Prod.* 34 (2011) 1035–1040.
 31. C. Cao, Z. Yang, L. Han, X. Jiang, G. Ji, Study on in situ analysis of cellulose, hemicelluloses and lignin distribution linked to tissue structure of crop stalk internodal transverse section based on FTIR microspectroscopic imaging, *Cellulose.* 22 (2015) 139–149.

32. K.M. Dokken, L.C. Davis, Infrared imaging of sunflower and maize root anatomy, *J. Agric. Food Chem.* 55 (2007) 10517–10530.
33. H. Yang, R. Yan, H. Chen, D.H. Lee, C. Zheng, Characteristics of hemicellulose, cellulose and lignin pyrolysis, *Fuel*. 86 (2007) 1781–1788.
34. P. Giudicianni, G. Cardone, R. Ragucci, Cellulose, hemicellulose and lignin slow steam pyrolysis: Thermal decomposition of biomass components mixtures, *J. Anal. Appl. Pyrolysis*. 100 (2013) 213–222. doi:10.1016/j.jaap.2012.12.026.
35. A.N. Shebani, A.J. Van Reenen, M. Meincken, The effect of wood extractives on the thermal stability of different wood species, *Thermochim. Acta*. 471 (2008) 43–50.
36. M. Poletto, A.J. Zattera, R. Santana, Structural differences between wood species: Evidence from chemical composition, FTIR spectroscopy, and thermogravimetric analysis, *J. Appl. Polym. Sci.* 126 (2012).
<http://onlinelibrary.wiley.com/doi/10.1002/app.36991/full> (accessed October 26, 2016).
37. C. Quan, A. Li, N. Gao, Thermogravimetric analysis and kinetic study on large particles of printed circuit board wastes, *Waste Manag.* 29 (2009) 2353–2360.